

# Nonlinear Discrete Optimisation of Reversible Steganographic Coding

Ching-Chun Chang

**Abstract**—Authentication mechanisms are at the forefront of defending the world from various types of cybercrime. Steganography can serve as an authentication solution by embedding a digital signature into a carrier object to ensure the integrity of the object and simultaneously lighten the burden of metadata management. However, steganographic distortion, albeit generally imperceptible to human sensory systems, might be inadmissible in fidelity-sensitive situations. This has led to the concept of reversible steganography. A fundamental element of reversible steganography is predictive analytics, for which powerful neural network models have been effectively deployed. As another core aspect, contemporary reversible steganographic coding is based primarily on heuristics and therefore worth further study. While attempts have been made to realise automatic coding with neural networks, perfect reversibility is still unreachable via such an unexplainable intelligent machinery. Instead of relying on deep learning, we aim to derive an optimal coding by means of mathematical optimisation. In this study, we formulate reversible steganographic coding as a nonlinear discrete optimisation problem with a logarithmic capacity constraint and a quadratic distortion objective. Linearisation techniques are developed to enable mixed-integer linear programming. Experimental results validate the near-optimality of the proposed optimisation algorithm benchmarked against a brute-force method.

**Index Terms**—Combinatorial mathematics, nonlinear discrete optimisation, reversible steganographic coding.

## I. INTRODUCTION

**S**TEGANOGRAPHY is the art and science of concealing information within a carrier object. This terminology encompasses a wide range of techniques and applications, including but not limited to covert communications [1], ownership identification [2], copyright protection [3], broadcast monitoring [4], and traitor tracing [5]. An important application of steganography is data authentication, which plays a vital role in cybersecurity. The advent of data-centric artificial intelligence is accompanied by cybersecurity concerns. It has been reported that machine-learning models are vulnerable to adversarial attacks such as invisible perturbations crafted to cause wrong decisions [6], poisonous data collected for re-training during deployment [7], and malware codes hidden in neural network parameters [8]. A proper authentication mechanism ensures that the integrity of data has not been undermined and that the identity of users has not been forged, thereby serving as a precaution against these insidious threats.

Digital signatures are an authentication mechanism based upon modern cryptography [9]. This mechanism can be incorporated into a trustworthy forensic camera in such a way that

photographs are generated and stored along with digital signatures [10]. However, storing such auxiliary metadata might entail the risk of accidental loss and mismanagement during the data lifecycle. Steganography can serve as a potential remedy to embed the auxiliary information about the data into the data itself in an invisible manner. Yet, steganography distortion, albeit generally imperceptible to human sensory systems, might not be admissible in some fidelity-sensitive situations such as legal proceedings, medical diagnosis, and military reconnaissance. This is where the notion of reversible computing comes into play [11]–[15].

A fundamental element of reversible steganography, in common with lossless compression, is predictive analytics [16]–[18]. Prediction error modulation is a cutting-edge reversible steganographic technique composed of an analytics module and a coding module [19]–[25]. The recent development of deep learning has advanced the frontier of reversible steganography. It has been reported that deep neural networks can be applied as powerful predictive models [26]–[29]. Despite an inspiring progress in the analytics module, the design of the coding module based largely on heuristics. While there are studies on *end-to-end* deep learning that attempts to use neural networks for automatic reversible computing, perfect reversibility cannot be promised [30]–[32]. From a certain point of view, it is hard for neural networks, as a monolithic black box, to learn the intricate logics of reversible computing. Explainability of intelligent machinery is an ongoing open research topic [33]–[36]. Therefore, it seems advisable to follow the *modular* framework at the time of writing.

This study is in pursuit of developing an optimal coding for reversible steganography. We model reversible steganographic coding as a mathematical optimisation problem and propose an optimisation algorithm for addressing the nonlinear nature of this problem. The remainder of this paper is organised as follows. Section II outlines the background regarding reversible steganography. Section III formulates the nonlinear discrete optimisation problem and discusses the complexity of brute-force search. Section IV presents linearisation techniques for tackling the nonlinear discrete optimisation problem. Section V analyses the optimality of solutions through simulation experiments. Section VI provides concluding remarks.

## II. BACKGROUND

Prediction error modulation is a reversible steganographic technique that consists of an analytics module and a coding module. The analytics module begins by splitting a cover image into the *context* and *query* sets, denoted by  $c$  and  $q$ ,

C.-C. Chang is with the University of Warwick, Coventry, UK (email: c.c.chang@warwickgrad.net).

Digital Object Identifier xx.xxxx/2022

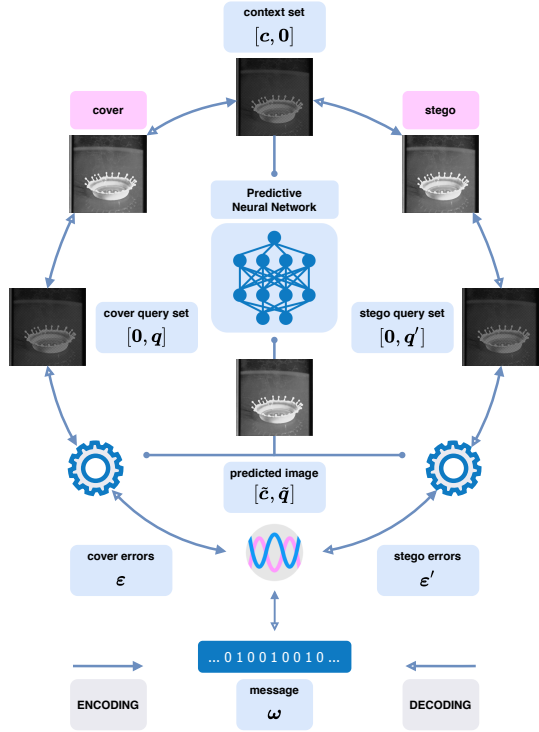


Fig. 1: Workflow of reversible steganography with prediction error modulation.

respectively. A conventional way is to divide pixels into two halves according to a chequered pattern. Then, a predictive model is applied to predict the query pixel intensities from the context pixel intensities. A contemporary practice is to employ an artificial neural network in computer vision. The coding module embeds a message  $\omega$  into the cover image by modulating the prediction errors  $\varepsilon = q - \tilde{q}$ . The modulated errors  $\varepsilon'$  is then added to the predicted intensities, causing distortion to the query pixels. The stego image is created by merging the context set  $c$  and the modulated query set  $q'$ . The decoding procedure is similar to the encoding procedure. It begins by predicting the query pixel intensities. Since the context set is kept unchanged, the prediction in the decoding phase is guaranteed to be identical to that in the encoding phase given the same predictive model. The message is extracted and the query set is recovered by demodulating the prediction errors. The image is reversed to its original state by merging the context set and the recovered query set. The procedures for encoding and decoding are depicted schematically in Figure 1 and also provided in Algorithms 1 and 2. We would like to note that the message may contain some auxiliary information for handling pixel intensity overflow. This paper does not go into details of every aspect of the stego-system; instead, our study focuses on mathematical optimisation of reversible steganographic coding.

### III. NONLINEAR DISCRETE OPTIMISATION

The essence of reversible steganographic coding is to designate one or multiple error values as the carrier and to determine how the values change to represent different message digits. A conventional heuristic for reversible steganographic coding is to choose the prediction errors of the peak frequency as the

---

#### Algorithm 1 Encoding

---

**Input:** cover,  $\omega$   
**Output:** stego

▷ analytics module  
 $[c, \tilde{q}] \leftarrow \text{split}(\text{cover})$   
 $[\tilde{c}, \tilde{q}] \leftarrow \text{predict}([c, \mathbf{0}])$

▷ coding module  
 $\varepsilon \leftarrow q - \tilde{q}$   
 $\varepsilon' \leftarrow \text{modulate}(\varepsilon, \omega)$   
 $q' \leftarrow \tilde{q} + \varepsilon'$   
stego  $\leftarrow \text{merge}(c, q')$

---



---

#### Algorithm 2 Decoding

---

**Input:** stego  
**Output:** cover,  $\omega$

▷ analytics module  
 $[c, q'] = \text{split}(\text{stego})$   
 $[\tilde{c}, \tilde{q}] = \text{predict}([c, \mathbf{0}])$

▷ coding module  
 $\varepsilon' = q' - \tilde{q}$   
 $[\varepsilon, \omega] = \text{demodulate}(\varepsilon')$   
 $q = \tilde{q} + \varepsilon$   
cover = merge( $c, q$ )

---

carrier. While the peak frequency implies the highest capacity, this capacity-greedy strategy is not necessarily optimal in terms of minimising distortion.

#### A. Problem Modelling

According to the typical law of error, the frequency of an error can be expressed as an exponential function of its numerical magnitude, disregarding sign [37]. In other words, the frequency distribution of prediction errors is expected to centre around zero. In general, a smaller absolute error tends to have a higher occurrence. A special exception is that the occurrence of zero might be lower than the occurrence of a certain absolute error considering that the latter is the sum of both positive and negative error occurrences. Consider an absolute error histogram as shown in Figure 2. The problem of reversible steganographic coding is to establish a mapping between the values in  $[0, n]$  and the values in  $[0, n + \vartheta]$ , where  $\vartheta$  denotes the extra quota and is typical defined to be less than or equal to the number of successive empty bins in the absolute error histogram. Encoding is a *one-to-many* mapping that links a cover value to one or more stego values. A message digit can only be represented if the connections are greater than one. Different cover value can never yield the same stego value in order to avoid an overlap between values and ambiguity

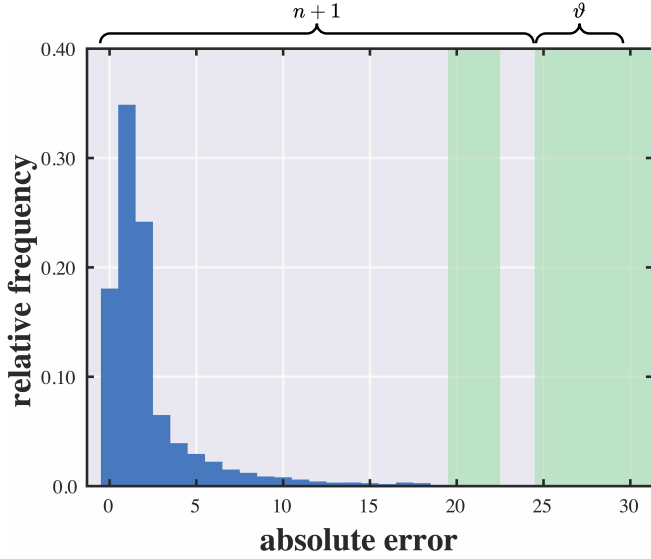


Fig. 2: Example of absolute error distribution with highlighted zero occurrences.

in decoding. Therefore, a cover value of non-zero occurrence may also be changed to a different stego value even if it is not assigned to represent any digit. We confine that each cover value can only be mapped to the nearest available stego values since a *non-cross* mapping reduces the problem dimension drastically. We choose to start from the mapping of value 0 to the mapping of value  $n$  because it is advisable to allocate a slighter cumulative distortion to a value of higher occurrence. An example of a cover/stego mapping is illustrated in Figure 3.

Let us denote by  $a_i$  the frequency of the value  $i$  and  $x_i$  the number of extra cover-to-stego links for the value  $i$ . The total number of links for the value  $i$  equals  $x_i + 1$ . The number of bits can be represented by the value  $i$  is  $\log_2(x_i + 1)$  and thus the capacity is computed by

$$\mathfrak{C} = \sum_{i=0}^n a_i \log_2(x_i + 1). \quad (1)$$

Given the total number of cover-to-stego links  $x_i$ , the probability of changing a cover value to each stego value is  $1/(x_i + 1)$ . The deviations of the first to the last stego value are  $y_i + 0$  to  $y_i + x_i$  respectively, where  $y_i$  denotes the sum of all the previous extra links (i.e. the cumulative deviation). Hence, the expected distortion in terms of the squared deviations is computed by

$$\mathfrak{D} = \sum_{i=0}^n a_i \left( \frac{(0 + y_i)^2 + \dots + (x_i + y_i)^2}{x_i + 1} \right), \quad (2)$$

where

$$y_i = \sum_{j=0}^{i-1} x_j. \quad (3)$$

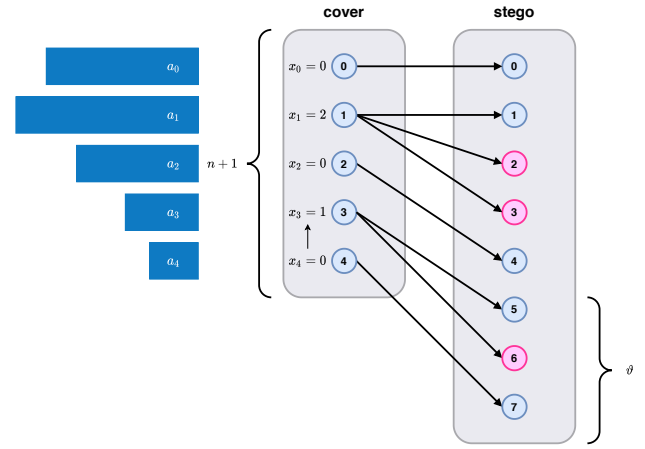


Fig. 3: Example of reversible steganographic coding.

We can simplify the algebraic expression by

$$\begin{aligned} & \frac{(0 + y_i)^2 + \dots + (x_i + y_i)^2}{x_i + 1} \\ &= \frac{(0^2 + 2y_i \cdot 0 + y_i^2) + \dots + (x_i^2 + 2y_i \cdot x_i + y_i^2)}{x_i + 1} \\ &= \frac{(0^2 + \dots + x_i^2) + 2y_i(0 + \dots + x_i) + y_i^2(x_i + 1)}{x_i + 1} \quad (4) \\ &= \frac{x_i(x_i + 1)(2x_i + 1)}{6(x_i + 1)} + \frac{2y_i x_i(x_i + 1)}{2(x_i + 1)} + \frac{y_i^2(x_i + 1)}{x_i + 1} \\ &= \frac{1}{3}x_i^2 + \frac{1}{6}x_i + x_i y_i + y_i^2. \end{aligned}$$

The reason for computing squared deviations rather than absolute deviations is that image quality is often measured by the peak signal-to-noise ratio (PSNR), which is defined via the mean squared error (MSE). Our goal is to solve for the decision variables  $x_i \in \{0, \dots, \vartheta\}$  that minimise the distortion objective subject to the capacity constraint. The sum of all the extra cover-to-stego links cannot exceed the quota  $\vartheta$ . To summarise, the mathematical optimisation problem for reversible steganographic coding is

$$\begin{aligned} \min \quad & \mathfrak{D} = \sum_{i=0}^n a_i \left( \frac{1}{3}x_i^2 + \frac{1}{6}x_i + x_i y_i + y_i^2 \right), \\ \text{s.t.} \quad & \mathfrak{C} = \sum_{i=0}^n a_i \log_2(x_i + 1) \geq \text{payload}, \\ & \sum_{i=0}^n x_i \leq \vartheta, \\ \text{var.} \quad & x_i \in \{0, \dots, \vartheta\}, \quad \forall i = 0, \dots, n. \end{aligned}$$

### B. Brute-Force Search

Brute-force search is a baseline method for benchmarking optimisation algorithms. The solution space that exhausts all possible combinations of the decision variables is equal to  $(\vartheta + 1)^{n+1} \in \mathcal{O}(c^n)$ . By taking into account of the quota constraint, we can reduce the solution space from the number of possible combinations to the number of feasible combinations. In number theory and combinatorics, the partition function

$\text{part}(t)$  computes the number of ways of writing  $t$  as a sum of positive integers in  $[1, t]$ . Let  $\mathbf{\Lambda}_t$  denote a matrix of  $\text{part}(t)$  rows and  $t$  columns that enumerates all possible partitions:

$$\mathbf{\Lambda}_t = \begin{bmatrix} \boldsymbol{\lambda}_1 \\ \vdots \\ \boldsymbol{\lambda}_{\text{part}(t)} \end{bmatrix} = \begin{bmatrix} \lambda_{1,1} & \cdots & \lambda_{1,t} \\ \vdots & \ddots & \vdots \\ \lambda_{\text{part}(t),1} & \cdots & \lambda_{\text{part}(t),t} \end{bmatrix}. \quad (5)$$

Each vector  $\boldsymbol{\lambda}_\ell$  represents a possible partition in which each element is the quantity of a candidate integer (i.e. the summand). For example,  $\mathbf{\Lambda}_2$ ,  $\mathbf{\Lambda}_3$  and  $\mathbf{\Lambda}_4$  are

$$\begin{bmatrix} 1 & 2 \\ 2 & 0 \\ 0 & 1 \end{bmatrix} \begin{matrix} \lambda_1 \\ \lambda_2 \end{matrix}, \quad \begin{bmatrix} 1 & 2 & 3 \\ 3 & 0 & 0 \\ 1 & 1 & 0 \\ 0 & 0 & 1 \end{bmatrix} \begin{matrix} \lambda_1 \\ \lambda_2 \\ \lambda_3 \end{matrix}, \quad \begin{bmatrix} 1 & 2 & 3 & 4 \\ 4 & 0 & 0 & 0 \\ 2 & 1 & 0 & 0 \\ 0 & 2 & 0 & 0 \\ 1 & 0 & 1 & 0 \\ 0 & 0 & 0 & 1 \end{bmatrix} \begin{matrix} \lambda_1 \\ \lambda_2 \\ \lambda_3 \\ \lambda_4 \\ \lambda_5 \end{matrix}.$$

The total number of feasible solutions can be calculated by adding up the number of feasible solutions given by each individual partition matrix from  $\mathbf{\Lambda}_1$  to  $\mathbf{\Lambda}_\vartheta$  (due to the quota constraint); that is,

$$\sum_{t=1}^{\vartheta} \text{feasible}(\mathbf{\Lambda}_t, n^*), \quad (6)$$

where  $n^* = n+1$  denotes the number of integers in  $[0, n]$ . For each matrix  $\mathbf{\Lambda}_t$ , the number of feasible solutions is computed by summing up the number of possible combinations given by each partition vector  $\boldsymbol{\lambda}_\ell$ , denoted by

$$\text{feasible}(\mathbf{\Lambda}_t, n^*) = \sum_{\ell=1}^{\text{part}(t)} \text{comb}(\boldsymbol{\lambda}_\ell, n^*). \quad (7)$$

A combination is a selection of values from a set of  $n^*$  values based on a given partition vector, as expressed by

$$\text{comb}(\boldsymbol{\lambda}_\ell, n^*) = \prod_{i=1}^t \binom{n^* - \sum_{j=1}^{i-1} \lambda_j^*}{\lambda_i^*}, \quad (8)$$

where  $\lambda_i^* = \lambda_{\ell,i}$  is the simplified notation regardless of the index of the partition vector. It is a product of  $t$  binomial coefficients and each term is to choose (and remove) an unordered subset of  $\lambda_i^*$  values from the remaining values in the set of  $n^*$  values. Let us take  $\mathbf{\Lambda}_3$  for example. The number of combinations for partition vectors  $\boldsymbol{\lambda}_1$ ,  $\boldsymbol{\lambda}_2$  and  $\boldsymbol{\lambda}_3$  are computed as follows:

$$\text{comb}(\boldsymbol{\lambda}_1, n^*) = \binom{n^*}{3} \binom{n^* - 3}{0} \binom{n^* - 3 - 0}{0},$$

$$\text{comb}(\boldsymbol{\lambda}_2, n^*) = \binom{n^*}{1} \binom{n^* - 1}{1} \binom{n^* - 1 - 1}{0},$$

$$\text{comb}(\boldsymbol{\lambda}_3, n^*) = \binom{n^*}{0} \binom{n^* - 0}{0} \binom{n^* - 0 - 0}{1}.$$

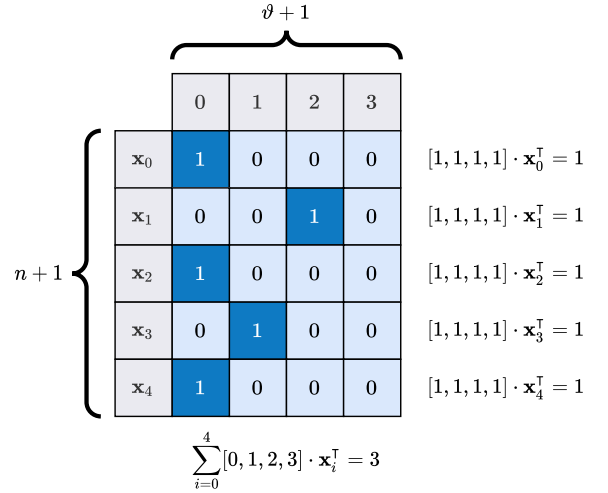


Fig. 4: Example of binary integer decision variable.

The number of combinations can be approximated by

$$\begin{aligned} & \prod_{i=1}^t \binom{n^* - \sum_{j=1}^{i-1} \lambda_j^*}{\lambda_i^*} \\ &= \binom{n^*}{\lambda_1^*} \binom{n^* - \lambda_1^*}{\lambda_2^*} \cdots \binom{n^* - \lambda_1^* - \lambda_2^* - \cdots - \lambda_{t-1}^*}{\lambda_t^*} \\ &= \frac{n^*!}{\lambda_1^*! (n^* - \lambda_1^*)!} \times \frac{(n^* - \lambda_1^*)!}{\lambda_2^*! (n^* - \lambda_1^* - \lambda_2^*)!} \times \cdots \\ &= \frac{n^*!}{\lambda_1^*! \lambda_2^*! \cdots \lambda_t^*!} \\ &= \frac{n^* (n^* - 1) (n^* - 2) \cdots (n^* - (\sum_{j=1}^t \lambda_j^* - 1))}{\lambda_1^*! \lambda_2^*! \cdots \lambda_t^*!} \\ &\leq \frac{n^* (n^* - 1) (n^* - 2) \cdots (n^* - (t - 1))}{\lambda_1^*! \lambda_2^*! \cdots \lambda_t^*!} \approx n^t. \end{aligned} \quad (9)$$

Hence, the complexity of this speed-up brute-force algorithm is approximately equal to

$$\sum_{t=1}^{\vartheta} \sum_{\ell=1}^{\text{part}(t)} \text{comb}(\boldsymbol{\lambda}_\ell, n^*) \approx \sum_{t=1}^{\vartheta} \text{part}(t) \cdot n^t \in \mathcal{O}(n^c). \quad (10)$$

#### IV. LINEARISATION

The difficulty of our optimisation problem lies in the nonlinear nature of the capacity constraint and the distortion objective. To apply off-the-shelf optimisation tools, we have to tackle these nonlinearities.

##### A. Logarithmic Capacity Constraint

The capacity constraint involves the calculation of logarithm of variables  $\log_2(x_i+1)$ . The logarithmic function is nonlinear. A useful linearisation trick is to remodel the problem with binary integer variables. We binarise each decision variable  $x_i$  with the domain  $[0, \vartheta]$  into a 0/1 vector or a one-hot vector of length  $\vartheta + 1$ , as illustrated in Figure 4. The vector consists of 0s with the exception of a single 1 of which the position indicates the value of  $x_i$ ; that is,

$$\mathbf{x}_i = [x_i^0, \dots, x_i^\vartheta] \in \{0, 1\}^{\vartheta+1}, \quad (11)$$

such that

$$\mathbb{1} \cdot \mathbf{x}_i^\top = 1, \quad \forall i = 0, \dots, n. \quad (12)$$

We can retrieve  $x_i$  by the dot product of vectors

$$x_i = [0, \dots, \vartheta] \cdot \mathbf{x}_i^\top = \mathbf{v}\mathbf{x}_i^\top. \quad (13)$$

Accordingly, the quota constraint becomes

$$\sum_{i=0}^n \mathbf{v}\mathbf{x}_i^\top \leq \vartheta. \quad (14)$$

In a similar manner, the logarithm can be derived by the dot product of vectors

$$\begin{aligned} \log_2(x_i + 1) &= [\log_2(0 + 1), \dots, \log_2(\vartheta + 1)] \cdot \mathbf{x}_i^\top \\ &= \mathbf{v}_{\log}\mathbf{x}_i^\top. \end{aligned} \quad (15)$$

Hence, we rewrite the capacity constraint as

$$\mathfrak{C} = \sum_{i=0}^n a_i \mathbf{v}_{\log}\mathbf{x}_i^\top. \quad (16)$$

### B. Quadratic Distortion Objective

The distortion objective involves three nonlinear terms  $x_i^2$ ,  $y_i^2$  and  $x_i y_i$ . These terms are quadratic functions of variables. The first term can be approached by the dot product as before; that is

$$x_i^2 = [0^2, \dots, \vartheta^2] \cdot \mathbf{x}_i^\top = \mathbf{v}_{\text{sq}}\mathbf{x}_i^\top. \quad (17)$$

The remaining two terms contain the partial sum of variables  $y_i$ , which is computed by

$$y_i = \sum_{j=0}^{i-1} \mathbf{v}\mathbf{x}_j^\top. \quad (18)$$

To linearise the univariate quadratic term  $y_i^2$  and the bivariate quadratic term  $x_i y_i$ , we introduce two non-negative continuous slack variables  $z_{y_i^2} \geq 0$  and  $z_{x_i y_i} \geq 0$ . Replacing the quadratic terms with the dot product and the slack variables results in a linear distortion objective

$$\mathfrak{D} = \sum_{i=0}^n a_i \left( \frac{1}{3} \mathbf{v}_{\text{sq}}\mathbf{x}_i^\top + \frac{1}{6} x_i + z_{x_i y_i} + z_{y_i^2} \right). \quad (19)$$

We begin by solving this mixed-integer linear programming problem, which does not yet reflect the quadratic terms regarding the cumulative distortion, and obtain an initial solution for  $\tilde{x}_i$ . The slack variables would be zeros because the objective is to minimise distortion. To make the slack variables reflect the quadratic terms properly, we add the following constraints

$$\begin{aligned} z_{y_i^2} &\geq y_i^2, \\ z_{x_i y_i} &\geq x_i y_i. \end{aligned} \quad (20)$$

In this way, we reformulate the problem with a nonlinear objective into the problem with a linear objective and nonlinear constraints. We make use of the solution obtained previously to linearise these nonlinear constraints and solve the mixed-integer linear programming problem iteratively. To begin with, we express the variables in terms of the previous solution:

$$\begin{aligned} x_i &= \tilde{x}_i + \delta_{x_i}, \\ y_i &= \tilde{y}_i + \delta_{y_i}, \end{aligned} \quad (21)$$

where  $\tilde{x}_i$  and  $\tilde{y}_i$  are treated as constants. Then, we apply the Taylor series to approximate the univariate quadratic term as

$$\begin{aligned} f(y_i) &= f(\tilde{y}_i + \delta_{y_i}) \\ &= f(\tilde{y}_i) + f'(\tilde{y}_i)\delta_{y_i} + \dots \\ &= \tilde{y}_i^2 + 2\tilde{y}_i\delta_{y_i} + \dots \\ &\approx \tilde{y}_i^2 + 2\tilde{y}_i(y_i - \tilde{y}_i) \\ &= 2\tilde{y}_i y_i - \tilde{y}_i^2, \end{aligned} \quad (22)$$

and similarly the bivariate quadratic term as

$$\begin{aligned} f(x_i, y_i) &= f(\tilde{x}_i + \delta_{x_i}, \tilde{y}_i + \delta_{y_i}) \\ &= f(\tilde{x}_i, \tilde{y}_i) + \frac{\partial f}{\partial x_i} \delta_{x_i} + \frac{\partial f}{\partial y_i} \delta_{y_i} + \dots \\ &= \tilde{x}_i \tilde{y}_i + \tilde{y}_i \delta_{x_i} + \tilde{x}_i \delta_{y_i} + \dots \\ &\approx \tilde{x}_i \tilde{y}_i + \tilde{x}_i (y_i - \tilde{y}_i) + \tilde{y}_i (x_i - \tilde{x}_i) \\ &= \tilde{x}_i y_i + \tilde{y}_i x_i - \tilde{x}_i \tilde{y}_i. \end{aligned} \quad (23)$$

As a result, the nonlinear constraints are transformed into the linear constraints

$$\begin{aligned} 2\tilde{y}_i y_i - z_{y_i^2} &\leq \tilde{y}_i^2, \\ \tilde{x}_i y_i + \tilde{y}_i x_i - z_{x_i y_i} &\leq \tilde{x}_i \tilde{y}_i. \end{aligned} \quad (24)$$

To recapitulate, the nonlinear discrete optimisation problem is approached by means of an iterative method that solves a mixed-integer linear programming problem with binary integer variables and non-negative continuous slack variables:

$$\begin{aligned} \min \quad \mathfrak{D} &= \sum_{i=0}^n a_i \left( \frac{1}{3} \mathbf{v}_{\text{sq}}\mathbf{x}_i^\top + \frac{1}{6} \mathbf{v}\mathbf{x}_i^\top + z_{x_i y_i} + z_{y_i^2} \right), \\ \text{s.t.} \quad \mathfrak{C} &= \sum_{i=0}^n a_i \mathbf{v}_{\log}\mathbf{x}_i^\top \geq \text{payload}, \\ &\sum_{i=0}^n \mathbf{v}\mathbf{x}_i^\top \leq \vartheta, \\ &\mathbb{1} \cdot \mathbf{x}_i^\top = 1, \quad \forall i = 0, \dots, n, \\ &2\tilde{y}_i y_i - z_{y_i^2} \leq \tilde{y}_i^2, \quad \forall i = 0, \dots, n, \\ &\tilde{x}_i y_i + \tilde{y}_i x_i - z_{x_i y_i} \leq \tilde{x}_i \tilde{y}_i, \quad \forall i = 0, \dots, n, \\ \text{var.} \quad \mathbf{x}_i &\in \{0, 1\}^{\vartheta+1}, \quad \forall i = 0, \dots, n, \\ &z_{y_i^2} \geq 0, \quad \forall i = 0, \dots, n, \\ &z_{x_i y_i} \geq 0, \quad \forall i = 0, \dots, n, \\ * \quad x_i &= \mathbf{v}\mathbf{x}_i^\top \quad \& \quad y_i = \sum_{j=0}^{i-1} \mathbf{v}\mathbf{x}_j^\top. \end{aligned}$$

## V. SIMULATION

We carry out experimental analysis on the optimality of the proposed method benchmarked against the brute-force method. The experimental setup is described as follows. We apply the residual dense network (RDN) as the predictive model [38]. This neural network model is characterised by a tangled labyrinth of residual and dense connections, and has its origin in low-level computer vision (e.g. super-resolution, denoising and deblurring). The model is trained on the BOSSbase dataset [39], which originated from an academic competition

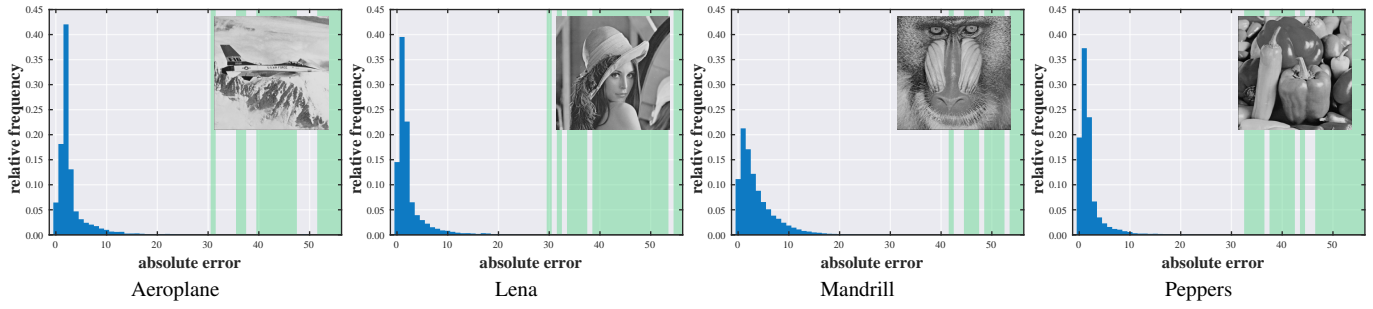


Fig. 5: Absolute error histograms with highlighted empty bins.

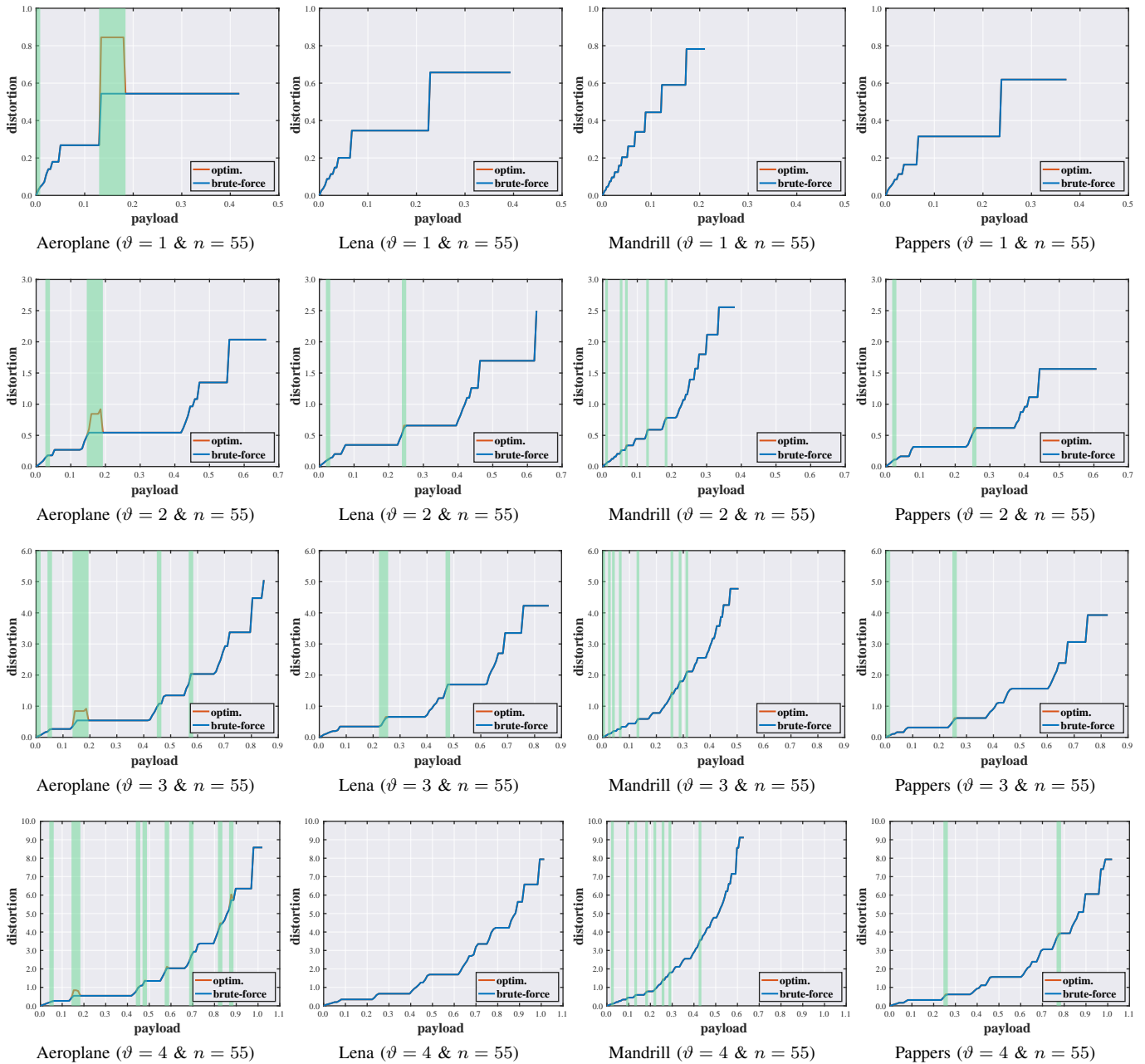


Fig. 6: Payload–distortion curves for optimality analysis against brute-force search.

for digital steganography. This dataset comprises a large collection of greyscale photographs covering a wide variety of subjects and scenes. The algorithms are tested on selected images from the USC-SIPI dataset [40]. All the images are resized to a resolution of  $256 \times 256$  pixels via Lanczos resampling [41]. The border pixels along with a half of the rest pixels are designated as the context. Accordingly, the number of query pixels equals  $(254 \times 254)/2$ . We display both distortion and capacity as divided by the number of query pixels.

Figure 5 shows the absolute error distribution for each test image. It is observed that most of the error values are within the range from about 30 to 50. We conservatively set  $n = 55$  in the sense that nearly every value of non-zero occurrence is included. We implement the algorithms with respect to different quota settings ( $\vartheta = 1, 2, 3, 4$ ). Figure 6 evaluates the performance of the proposed optimisation algorithm. Each point of the curve indicates the minimum distortion of a solution under a specific capacity constraint. In the vast majority of cases, the solutions found by the proposed method are identical to those given by the brute-force method. When failing to find the optimal solutions, the reached objective values are within a small distance from the optimal ones. Hence, even though the optimal solutions cannot be always guaranteed, the results suggest that the proposed method can achieve a near-optimal performance.

## VI. CONCLUSION

This paper studies a mathematical optimisation problem in reversible steganography. We formulate the prediction error coding as a nonlinear discrete optimisation problem. The objective is to minimise distortion under a constraint on capacity. We discuss the complexity of a brute-force method and the linearisation techniques for logarithmic capacity constraint and quadratic distortion objective. The problem is transformed into an iterative mixed-integer linear programming problem with binary integer variables and slack variables. Our simulation results validate the near-optimality of the proposed algorithm.

## REFERENCES

- [1] J. Fridrich, M. Goljan, P. Lisonek, and D. Soukal, "Writing on wet paper," *IEEE Trans Signal Process.*, vol. 53, no. 10, pp. 3923–3935, 2005.
- [2] I. J. Cox, J. Kilian, F. T. Leighton, and T. Shamoon, "Secure spread spectrum watermarking for multimedia," *IEEE Trans. Image Process.*, vol. 6, no. 12, pp. 1673–1687, 1997.
- [3] M. Barni, F. Bartolini, V. Cappellini, and A. Piva, "A DCT-domain system for robust image watermarking," *Signal Process.*, vol. 66, no. 3, pp. 357–372, 1998.
- [4] G. Depovere, T. Kalker, J. Haitsma, M. Maes, L. de Strycker, P. Termont, J. Vandeweghe, A. Langell, C. Alm, P. Norman, G. O'Reilly, B. Howes, H. Vaanholt, R. Hintzen, P. Donnelly, and A. Hudson, "The VIVA project: Digital watermarking for broadcast monitoring," in *Proc. Int. Conf. Image Process. (ICIP)*, Kobe, Japan, 1999, pp. 202–205.
- [5] Shan He and Min Wu, "Joint coding and embedding techniques for multimedia fingerprinting," *IEEE Trans. Inf. Forensics Secur.*, vol. 1, no. 2, pp. 231–247, 2006.
- [6] I. Goodfellow, J. Shlens, and C. Szegedy, "Explaining and harnessing adversarial examples," in *Proc. Int. Conf. Learn. Represent. (ICLR)*, San Diego, CA, USA, 2015, pp. 1–11.
- [7] L. Muñoz González, B. Biggio, A. Demontis, A. Paudice, V. Wongrasamee, E. C. Lupu, and F. Roli, "Towards poisoning of deep learning algorithms with back-gradient optimization," in *Proc. ACM Workshop Artif. Intell. Secur. (AISec)*, Dallas, TX, USA, 2017, pp. 27–38.
- [8] T. Liu, Z. Liu, Q. Liu, W. Wen, W. Xu, and M. Li, "StegoNet: Turn deep neural network into a stegomalware," in *Proc. Annu. Comput. Secur. Appl. Conf. (ACSAC)*, Austin, TX, USA, 2020, pp. 928–938.
- [9] R. L. Rivest, A. Shamir, and L. Adleman, "A method for obtaining digital signatures and public-key cryptosystems," *Commun. ACM*, vol. 21, no. 2, pp. 120–126, 1978.
- [10] G. Friedman, "The trustworthy digital camera: Restoring credibility to the photographic image," *IEEE Trans. Consum. Electron.*, vol. 39, no. 4, pp. 905–910, 1993.
- [11] J. Fridrich, M. Goljan, and R. Du, "Invertible authentication," in *Proc. SPIE Conf. Secur. Watermarking Multimedia Contents (SWMC)*, San Jose, CA, USA, 2001, pp. 197–208.
- [12] C. De Vleeschouwer, J.-F. Delaigle, and B. Macq, "Circular interpretation of bijective transformations in lossless watermarking for media asset management," *IEEE Trans. Multimedia*, vol. 5, no. 1, pp. 97–105, 2003.
- [13] A. M. Alattar, "Reversible watermark using the difference expansion of a generalized integer transform," *IEEE Trans. Image Process.*, vol. 13, no. 8, pp. 1147–1156, 2004.
- [14] S. Lee, C. D. Yoo, and T. Kalker, "Reversible image watermarking based on integer-to-integer wavelet transform," *IEEE Trans. Inf. Forensics Secur.*, vol. 2, no. 3, pp. 321–330, 2007.
- [15] G. Coatrieux, W. Pan, N. Cuppens-Boulahia, F. Cuppens, and C. Roux, "Reversible watermarking based on invariant image classification and dynamic histogram shifting," *IEEE Trans. Inf. Forensics Secur.*, vol. 8, no. 1, pp. 111–120, 2013.
- [16] C. E. Shannon, "A mathematical theory of communication," *Bell Syst. Tech. J.*, vol. 27, no. 3, pp. 379–423, 1948.
- [17] J. Rissanen, "Universal coding, information, prediction, and estimation," *IEEE Trans. Inf. Theory*, vol. 30, no. 4, pp. 629–636, 1984.
- [18] M. Weinberger and G. Seroussi, "Sequential prediction and ranking in universal context modeling and data compression," *IEEE Trans. Inf. Theory*, vol. 43, no. 5, pp. 1697–1706, 1997.
- [19] M. U. Celik, G. Sharma, A. M. Tekalp, and E. Saber, "Lossless generalized-LSB data embedding," *IEEE Trans. Image Process.*, vol. 14, no. 2, pp. 253–266, 2005.
- [20] D. M. Thodi and J. J. Rodriguez, "Expansion embedding techniques for reversible watermarking," *IEEE Trans. Image Process.*, vol. 16, no. 3, pp. 721–730, 2007.
- [21] M. Fallahpour, "Reversible image data hiding based on gradient adjusted prediction," *IEICE Electron. Exp.*, vol. 5, no. 20, pp. 870–876, 2008.
- [22] V. Sachnev, H. J. Kim, J. Nam, S. Suresh, and Y.-Q. Shi, "Reversible watermarking algorithm using sorting and prediction," *IEEE Trans. Circuits Syst. Video Technol.*, vol. 19, no. 7, pp. 989–999, 2009.
- [23] X. Li, B. Yang, and T. Zeng, "Efficient reversible watermarking based on adaptive prediction-error expansion and pixel selection," *IEEE Trans. Image Process.*, vol. 20, no. 12, pp. 3524–3533, 2011.
- [24] I. Dragoi and D. Coltuc, "Local prediction based difference expansion reversible watermarking," *IEEE Trans. Image Process.*, vol. 23, no. 4, pp. 1779–1790, 2014.
- [25] H. J. Hwang, S. Kim, and H. J. Kim, "Reversible data hiding using least square predictor via the LASSO," *EURASIP J. Image Video Process.*, vol. 2016, no. 1, pp. 42: 1–12, 2016.
- [26] C.-C. Chang, "Adversarial learning for invertible steganography," *IEEE Access*, vol. 8, pp. 198 425–198 435, 2020.
- [27] R. Hu and S. Xiang, "CNN prediction based reversible data hiding," *IEEE Signal Process. Lett.*, vol. 28, pp. 464–468, 2021.
- [28] C.-C. Chang, "Neural reversible steganography with long short-term memory," *Secur. Commun. Netw.*, vol. 2021, pp. 5 580 272:1–14, 2021.
- [29] C.-C. Chang, X. Wang, S. Chen, I. Echizen, V. Sanchez, and C.-T. Li, "Deep learning for predictive analytics in reversible steganography," arXiv, 2022.
- [30] K.-H. Jung, Z. Zhang, G. Fu, F. Di, C. Li, and J. Liu, "Generative reversible data hiding by image-to-image translation via GANs," *Secur. Commun. Netw.*, vol. 2019, pp. 4 932 782:1–10, 2019.
- [31] X. Duan, K. Jia, B. Li, D. Guo, E. Zhang, and C. Qin, "Reversible image steganography scheme based on a U-Net structure," *IEEE Access*, vol. 7, pp. 9314–9323, 2019.
- [32] S.-P. Lu, R. Wang, T. Zhong, and P. L. Rosin, "Large-capacity image steganography based on invertible neural networks," in *Proc. IEEE/CVF Conf. Comput. Vis. Pattern Recognit. (CVPR)*, virtual, 2021, pp. 10 816–10 825.
- [33] D. Castelvecchi, "Can we open the black box of AI?" *Nature*, vol. 538, no. 7623, pp. 20–23, 2016.
- [34] L. H. Gilpin, D. Bau, B. Z. Yuan, A. Bajwa, M. Specter, and L. Kagal, "Explaining explanations: An overview of interpretability of machine

- learning,” in *IEEE Int. Conf. Data Sci. Adv. Anal. (DSAA)*, Turin, Italy, 2018, pp. 80–89.
- [35] A. Barredo Arrieta, N. Díaz-Rodríguez, J. Del Ser, A. Bennetot, S. Tabik, A. Barbado, S. García, S. Gil-Lopez, D. Molina, R. Benjamins, R. Chatila, and F. Herrera, “Explainable artificial intelligence (XAI): Concepts, taxonomies, opportunities and challenges toward responsible AI,” *Inf. Fusion*, vol. 58, pp. 82–115, 2020.
- [36] W. Samek, G. Montavon, S. Lapuschkin, C. J. Anders, and K.-R. Müller, “Explaining deep neural networks and beyond: A review of methods and applications,” *Proc. IEEE*, vol. 109, no. 3, pp. 247–278, 2021.
- [37] E. B. Wilson, “First and second laws of error,” *J. Amer. Statist. Assoc.*, vol. 18, no. 143, pp. 841–851, 1923.
- [38] Y. Zhang, Y. Tian, Y. Kong, B. Zhong, and Y. Fu, “Residual dense network for image super-resolution,” in *Proc. IEEE/CVF Conf. Comput. Vis. Pattern Recognit. (CVPR)*, Salt Lake City, UT, USA, 2018, pp. 2472–2481.
- [39] P. Bas, T. Filler, and T. Pevný, “Break our steganographic system: The ins and outs of organizing BOSS,” in *Proc. Int. Workshop Inf. Hiding (IH)*, Prague, Czech Republic, 2011, pp. 59–70.
- [40] A. G. Weber, “The USC-SIPI image database: Version 5,” USC Viterbi School Eng., Signal Image Process. Inst., Los Angeles, CA, USA, Tech. Rep. 315, 2006.
- [41] C. E. Duchon, “Lanczos filtering in one and two dimensions,” *J. Appl. Meteorol.*, vol. 18, no. 8, pp. 1016–1022, 1979.

PLACE  
PHOTO  
HERE

**Ching-Chun Chang** received his PhD in Computer Science from the University of Warwick, UK, in 2019. He engaged in a short-term scientific mission supported by European Cooperation in Science and Technology Actions at the Faculty of Computer Science, Otto-von-Guericke-Universität Magdeburg, Germany, in 2016. He was granted the Marie-Curie fellowship and participated in a research and innovation staff exchange scheme supported by Marie Skłodowska-Curie Actions at the Department of Electrical and Computer Engineering, New Jersey Institute of Technology, USA, in 2017. He was a Visiting Scholar with the School of Computer and Mathematics, Charles Sturt University, Australia, in 2018, and with the School of Information Technology, Deakin University, Australia, in 2019. He was a Research Fellow with the Department of Electronic Engineering, Tsinghua University, China, in 2020. His research interests include steganography, watermarking, forensics, biometrics, cybersecurity, applied cryptography, image processing, computer vision, natural language processing, computational linguistics, machine learning and artificial intelligence.